

Reusable Manganese compounds containing pyrazole-based ligands for olefin epoxidation reactions

Ester Manrique,^a Albert Poater,^a Xavier Fontrodona,^a Miquel Solà,^a Montserrat Rodríguez^{*a} and Isabel Romero^{*a}

^aDepartament de Química, Institut de Química Computacional i Catàlisi and Serveis Tècnics de Recerca, Universitat de Girona, Campus de Montilivi, E-17071 Girona, Spain.

Abstract

We describe the synthesis of new manganese (II) and manganese (III) complexes containing the bidentate ligands 2-(3-pyrazolyl)pyridine, *pypz-H*, and 3(5)-(2-hydroxyphenyl)pyrazole, *HOpmpz-H*, with formula $[\text{MnX}_2(\text{pypz-H})_2]$ ($\text{X} = \text{Cl}^-$, **1**, CF_3SO_3^- , **2**, OAc^- , **3** or NO_3^- (**4**)), $[\text{MnCl}_2(\text{pypz-H})(\text{H}_2\text{O})_2]$, **5**, or $[\text{MnCl}(\text{Opmpz-H})_2]$, **6**. All the complexes have been characterized through analytical, spectroscopic and electrochemical techniques. Single X-ray structure analysis revealed a six-coordinated Mn(II) ion in complexes **1–5**, and a five-coordinated Mn(III) ion in complex **6**. Compound **5** is the first co-crystal of Mn(II) containing Cl and H_2O ligands together with bidentate nitrogen ligands. The catalytic activity of complexes **1–6** has been tested with regard to the epoxidation of styrene and, in the case of **1**, **5** and **6**, other alkenes have been epoxidized using peracetic acid as oxidant in different media, among which glycerol, a green solvent never used in epoxidation reaction using peracetic acid as oxidant. The catalysts show moderate to high conversions and selectivities towards the corresponding epoxides. For complexes **1**, **5** and **6**, a certain degree of *cis*→*trans* isomerization is observed in the case of *cis*- β -methylstyrene. These observations have been explained through computational calculations. The reutilization of catalysts **1** and **6** for the epoxidation of alkenes has been evaluated in [bmim]:acetonitrile mixture (bmim = 1-butyl-3-methylimidazolium), allowing the effective recyclability of the catalytic system and keeping high conversion and selectivity values up to 12 successive runs, in all cases.

KEYWORDS: manganese/ oxidation catalysis/ ionic liquids/ reaction pathway/ recyclability

Introduction

Metal-catalysed oxidation is one of the most important transfer reactions in chemistry and biology.¹ Olefin epoxidation has received considerable interest from both academics and industry since epoxides play an important role as intermediates and building blocks in inorganic synthesis and material science.² It has been shown that this reaction proceeds via oxo- or peroxy-metal intermediates with the participation in most cases of multiple active oxidants;³ however, the need to understand more about this mechanism demands the search for efficient, robust and recyclable catalysts. Transition-metal complexes with ligands containing nitrogen as donor atoms constitute an important class of coordination compounds that are able to perform a wide range of transformations. Nitrogen-based ligands have well-known advantages such as chemical robustness or rich coordination chemistry in combination with inexpensive first-row transition metal (useful for oxidation catalysis) as manganese where the most developed systems are those based on sp²-hybridized nitrogen-donor atoms such as chiral oxazolines⁴ or pyridines,⁵ porphyrines⁶ and Salen ligands.⁷ Manganese complexes containing bipyridine (and derivatives) have shown to be good catalysts for the epoxidation of alkenes,⁸ and the use of mixed ligands as pyridine/pyrazole or phenol/pyrazole is expected to generate also active compounds for this reaction. Moreover, although the magnetic and thermal properties of manganese compounds containing pyrazole-pyridine ligands (such as 2-(3-pyrazolyl)pyridine, *pypz-H*, or phenol-pyrazole ligands, such as 3(5)-(2'-hydroxyphenyl)pyrazole, *HOpHz-H*) have been extensively described,⁹ they have never been studied as potential catalysts in oxidation reactions.

Chemical transformations, as well as other industrial productive processes, are experiencing a profound transformation to meet sustainability criteria, moving from old methods to new ones developed in agreement with green chemistry principles.¹⁰ Substitution of harmful and hazardous chemicals with others more compatible with human health and the environment is mandatory, and among these the solvent replacement is especially important since amounts of solvents are usually much larger than those of reagents and products. In this context, new solvents should exhibit small environmental impact, no toxicity and no volatility to meet the demands for sustainability.¹¹ Glycerol derivatives are promising solvents in this respect, and glycerol itself appears as a valuable green solvent that is produced as a concomitant product in biodiesel preparation.¹² Glycerol derivatives have been studied in some epoxidation reactions using hydrogen peroxide as oxidant,^{11b,13} but their application is limited so far.

On the other hand, heterogeneization and reuse of catalysts are fields of unquestionable importance

especially towards their application in large-scale processes.¹⁴ In this context, room temperature ionic liquids (RTILs) have received in recent years a good deal of attention as potential alternative solvents or co-solvents in catalysis¹⁵ given their potential benefits, particularly the simplicity of product separation and also the easy recyclability of the catalyst. Numerous possible combinations of cations and anions offer convenient ways to fine-tune the physicochemical properties of ILs such as polarity, viscosity and miscibility with others reagents. Most metal catalysts are soluble in ILs without modification of the ligands, and usually the non-coordinating anions of ILs leave the active sites of catalysts available for interaction with the substrates. Recently our group has described the epoxidation activity of two Mn^{II} complexes containing bipyridyl ligands^{8a} in ionic liquid/solvent media that constitute some of the scarce systems evaluated to date as epoxidation catalysts in such media.^{16,17}

With all this in mind, in this work we describe the synthesis and full characterization of new compounds based on Mn^{II} and Mn^{III} using the pyrazolic ligands 2-(3-pyrazolyl)pyridine, *pypz-H*, and 3(5)-(2-hydroxyphenyl)pyrazole, *HOpHz-H*, together with different monodentate ligands. Compounds **1-4** (with general formula [MnX₂(pypz-H)₂], where X is a monodentate anionic ligand) and **6**, [MnCl(Ophpz-H)₂], are obtained as a sole geometrical isomer whereas **5**, [MnCl₂(pypz-H)(H₂O)₂], is a cocrystal that contains two different isomers (see below the structural description). We have also studied the performance of the complexes as catalysts in the epoxidation of styrene with peracetic acid, and the performance of chlorido compounds **1**, **5** and **6** in the epoxidation of other olefins in different media among which glycerol, a green solvent never used in epoxidation reaction using peracetic acid as oxidant. Finally, we have investigated the reutilization and activity of catalysts **1** and **6** in ionic liquid:solvent media, a system that constitutes the first example of pyrazolic Mn^{II} and Mn^{III} complexes tested under such conditions. A degree of *cis*→*trans* isomerization is observed experimentally for the catalysts in the epoxidation of *cis*-β-methylstyrene in acetonitrile and this fact has been supported by computational calculations.

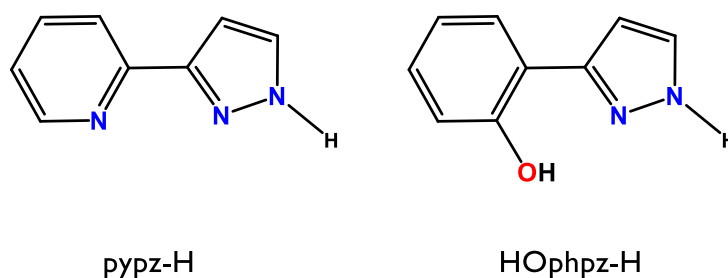


Chart 1. Drawing of the two pyrazolic ligands

Results and discussion

Synthesis and Structure

The synthetic strategy followed for the preparation of Mn^{II} complexes **1-5**, containing the *pypz-H* ligand, and complex **6**, containing the *HOphpz-H* ligand, is outlined in Scheme 1. Different Mn(II) salts are used as starting materials and then the corresponding ligand is added stepwise for the preparation of complexes **1-6**.

When an ethanolic solution of ligand *pypz-H* is added to MnCl₂ dissolved in ethanol with a metal:ligand ratio 1:2.5, the complex [MnCl₂(*pypz-H*)₂], **1**, is obtained in good yield and it can be crystallized by slow evaporation of the corresponding solution. However, when the metal:ligand ratio is 1:1 complex [MnCl₂(*pypz-H*)(H₂O)₂], **5**, containing only one unit of the bidentate ligand, is isolated. A metal:ligand ratio of 1:2 is used to obtain the mononuclear compounds [Mn(CF₃SO₃)₂(*pypz-H*)₂], **2**, [Mn(OAc)₂(*pypz-H*)₂], **3**, and [Mn(NO₃)₂(*pypz-H*)₂], **4**, starting from the corresponding Mn(II) salts. Finally, the reaction of MnCl₂ with *HOphpz-H* ligand in a metal:ligand ratio of 1:2 and in the presence of NaOH results in the formation of the Mn(III) complex [MnCl(O*phpz-H*)₂], **6**. In this case, the deprotonation of the ligand upon coordination leads to the subsequent oxidation of the Mn center facilitated by the increased σ-donor capacity of the ligand.

The crystal structures of all complexes have been solved by X-ray diffraction analysis. Crystallographic data and selected bond distances and angles for compounds **1-6** are presented in Table S1 and S2 (see supporting information section). ORTEP plots with the corresponding atom labels for the X-ray structures of all compounds are presented in Figure 1. Crystal structures of mononuclear compounds **1-4**, containing the *pypz-H* ligand, reveal in all cases a distorted octahedral geometry around the metal, where Mn(II) ion is coordinated by four nitrogen atoms of two *pypz-H* ligands and two anionic monodentate ligands adopting a *cis* configuration. Compound **3** is, to the best of our knowledge, the first described mononuclear Mn(II) compound where acetate groups are acting as monodentate ligands adopting a *cis* configuration around the metal. It is noticeable that in the four complexes the respective anionic ligands are situated *trans* to the pyridyl ring of each *pypz-H* ligand, which is consistent with the higher Lewis basicity of pyrazole as compared to pyridine. Mn-N bond lengths also manifest this *trans* effect since the average Mn-N_{pyridyl} bond distances for each compound are longer than the corresponding Mn-N_{pyrazole}, where two pyrazole rings are mutually in *trans* position. The Mn-Cl, Mn-O_{triflate}, Mn-O_{acetate} and Mn-O_{nitrate} bond distances are comparable to those found in similar Mn(II) compounds.¹⁸ Metal-ligand angles

deviate significantly from the ideal value of 90° or 180° characteristic of a regular octahedron due to the spatially constrained nature of the *pypz-H* ligand coordinated to the metal ($N_{pz}\text{-Mn-}N_{py}$ = 70.87°(**1**); 72.77°(**2**); 71.07 °(**3**); 71.95°(**4**)); also, $N_{pz}\text{-Mn-}N_{pz}$ bond angles are significantly less than 180°). This deviation is more significant for the nitrate compound **4**, and consequently hydrogen-bonding interactions take place between the coordinated oxygen atoms and the closest pyrazolic hydrogen atoms ($O(1)\text{-H}(3)$ = 2.786 Å; $O(4)\text{-H}(6)$ = 2.721 Å), whereas in compounds **2** and **3** strong hydrogen-bonding are also present but involves the oxygen atoms not coordinated to the metal center.

The spatial disposition of two *pypz-H* ligands and two monodentate ligands in an octahedral environment, as is the case of complexes **1-4**, could potentially lead to a set of eight different isomers (including three pairs of enantiomers, see Scheme S1). The nomenclature *trans* or *cis* for the isomers refers to the relative position of the two monodentate X ligands and also to the relative position of the pyridyl or pyrazolyl rings of the two *pypz-H* ligands in each case, as indicated in Scheme S1. However, as evidenced by the X-ray structures of the complexes (Figure 1), the enantiomeric pair Δ/Λ *cis-X-trans-pz* is the isomer obtained in all cases. The specificity towards this isomer can be interpreted in terms of the presence of two intramolecular H-bonds between the monodentate ligands (X) and the pyrazole H atoms in *cis* to each monodentate ligand. These hydrogen bonding interactions also determine the packing of the molecules within the solid tridimensional network (see Figure S1). In complex **1**, weak intramolecular hydrogen bonding interactions are observed between the Cl ligands and the pyrazolic hydrogen atoms ($H(2b)\text{-Cl}(1)$ = 3.148 Å, see Figure 1 for the numbering scheme). The triflate compound **2** displays two strong intramolecular H-bonding between the non-coordinated oxygen atoms and the hydrogen atoms of the pyrazole ring ($O(2)\text{-H}(6a)$ = 2.091 Å; $O(5)\text{-H}(3b)$ = 2.120 Å) whereas for the acetate compound **3**, a strong intramolecular H-bonding is present between the uncoordinated O(2) atom and H(1), 2.073 Å. The nitrate compound **4** displays a high distortion from the ideal octahedral geometry (presenting an environment between octahedral and trigonal prismatic) with intramolecular interactions between the pyrazolic hydrogen atoms and the coordinated oxygen nitrate atoms, as we have previously mentioned.

The X-ray structure of complex **5** (Figure 1) is a co-crystal that contains two isomers: *trans-Cl,cis-H₂O* and *cis-Cl,trans-H₂O*, where two chlorido and two aqua ligands are mutually placed *trans* or *cis*, and π -stacking interactions between the *pypz-H* rings of the two isomers are present. In both isomers, a distorted octahedral geometry around the metal is observed, where Mn(II) ions are coordinated by two nitrogen atoms of one *pypz-H* ligand, two chloride ions and two oxygen atoms from terminal aqua ligands. To the

best of our knowledge, this compound is the first reported co-crystal of Mn(II) containing Cl and H₂O ligands and also the first one containing a bidentate nitrogen ligand together with two Cl and two H₂O ligands; some compounds are described in the literature that contain Cl and H₂O ligands but together with two monodentate nitrogen ligands¹⁹ and, in all the cases, nitrogen ligands are arranged in *trans* position with respect to each other.

The spatial disposition of four monodentate ligands and one bidentate ligand in octahedral environment, as is the case of complex **5**, could potentially lead to a set of six different stereoisomers (including two pairs of enantiomers) as depicted in Scheme S3. The nomenclature *trans* or *cis* refers to the relative position of two identical monodentate ligands (Cl or H₂O) and, in the case of *cis,cis* isomers, the ligand indicated in brackets at the end is the one placed in *trans* with regard to the pyrazole ring. As stated above, complex **5** is attained as an equimolar mixture of the two *cis,trans* isomers depicted in Scheme S2, and this behaviour is most likely explained by supramolecular interactions taking place within the crystal packing. Weak intermolecular interactions such as hydrogen bonding and aryl-aryl stacking interactions play important roles in the creation of a variety of molecular architectures for molecular self-assembly and recognition.²⁰ The geometries of ligands also influence the topologies of their metal complexes, especially for low-nuclearity coordination complexes.²¹ In this context, the specificity towards the isomers formed in complex **5** can be interpreted in terms of the presence of strong intermolecular H-bonding (O-H...Cl contacts around 2.3 Å) together with π -stacking interactions between the pyridine and pyrazole rings that establish connections between the two isomers and favor their co-crystallization under the 1:1 ratio found. Also, weak intramolecular H-bonding interactions take place between the hydrogen atoms of the *pypz-H* ligand and the monodentate Cl or H₂O ligands disposed in *cis* configuration and located at the equatorial plane defined by the *pypz-H* ligand (N_{pz}-H...Cl, 3.094 Å, N_{py}-H...O H, 2.883 Å). These intramolecular hydrogen bonding interactions together with the spatially constrained nature of the *pypz-H* ligand coordinated to the metal are responsible for the octahedral geometry distortion around the Mn(II) ions (N_{pz}-Mn(1)-N_{py}= 71.51°; N_{pz}-Mn(1a)-N_{py}= 72.73°). The resulting packing of this compound presents a compact structure made by alternate layers of the two different isomers, *trans*-Cl-*cis*-H₂O and *cis*-Cl-*trans*-H₂O (see Figure S2).

Complex **6** can also be obtained as different isomers as depicted in the supporting information (Scheme S3), but a single isomer has been observed (Figure 1) probably due, as is the case for complexes **1-4**, to the presence of two H-bonding N-H...O interactions between the two *Ophpz-H* ligands that are not found

in the rest of isomers. The geometry around the Mn(III) ion is a distorted square-pyramid with a τ index of 0.20 ($\tau = 0$ for a square-pyramid, and $\tau = 1$ for trigonal bipyramid),²² where the base is defined by the two bidentate ligands and the monodentate chloride ion occupies the apical position. The Mn-O and the Mn-N average bond lengths are 1.85 Å and 1.97 Å respectively and are shorter than the Mn-Cl bond (2.45 Å) which indicates that the chloride ion interacts with Mn(III) in a weaker way than the donor atoms from the hydroxyphenyl pyrazole ligands, as expected. However, the Mn-Cl bond is shorter than the analogous Mn-X distance found in a similar structure that contains a bromo ligand instead of Cl, due to the smaller ionic radius and larger electronegativity of Cl⁻ when compared to Br⁻.^{9a} This fact is also reflected in the distortion of the coordination geometry, where the distance of the manganese(III) ion from the N₂O₂ mean plane is 0.242 Å (in the reported structure with a bromo ligand the distance of Mn with regard to the analogous plane is 0.337 Å). The average of the two intraligand O-Mn-N angles is slightly smaller than 90° (89.07°). The structure contains also intramolecular H-bonding interactions between the O(1) and O(2) oxygen atoms and the pyrazole H(1) and H(3) hydrogen atoms (Figure 1 and S3). The packing of **6**, organized in zig-zag ladder-like chains (see Figure S3), presents π -stacking interactions together with intermolecular H-bonding between Cl and the pyrazole N-H atoms, (N(1)-H(1)⋯Cl(1) = 3.207 Å). These interactions are stronger than in other compounds previously reported in the literature.⁹

Electrochemical properties

The redox potentials of complexes **1-6** were determined by cyclic voltammetry (CV) and differential pulse voltammetry (DPV) in CH₃CN containing 0.1 M of *n*-Bu₄NPF₆ (TBAH) as supporting electrolyte using Ag/AgNO₃ as reference electrode. The voltammograms obtained are shown in Figure 2 and in the supporting information section (Figure S4). The CV of complexes **1** and **5** (Figures 2 and S4 respectively) exhibit a one-electron quasi-reversible redox wave at potential values of $E_{1/2} = 0.63$ V (**1**) and 0.66 V (**5**) corresponding to the Mn^{III}/Mn^{II} system. In contrast, for compounds **2**, **3**, and **4** the CV experiments do not display well defined redox processes and thus DPV experiments have been carried out to determine the potential values more precisely (Figure S4), yielding $E_{1/2}$ values (in V) of 0.72 (**2**), 0.74 (**3**) and 0.73 (**4**). As can be observed, triflate (**2**), acetate (**3**) and nitrate (**4**) compounds are oxidised at higher potentials than the structurally similar chlorido complex **1**, which can be explained in terms of the stronger electron-donating capacity of chlorido ligands compared to the above mentioned anions.

Regarding the pentacoordinated complex **6**, an irreversible oxidation process is found at $E_{p,a} = 0.95$ V, which can be assigned to the Mn(IV/III) redox pair. This assignment has been carried out on the basis of a

bulk electrolysis (not shown) performed at an applied potential of 0.5 V after which the initial Mn(III) complex remains unchanged. We have not observed any wave corresponding to the Mn(III/II) redox pair in the potential range from -0.6 to 1.5 V, indicating that the coordination of three anionic ligands to Mn highly destabilizes the Mn(II) oxidation state.

The monoelectronic nature of the wave was confirmed in compound **1** by performing a bulk electrolysis of a 1 mM solution of the complex in acetonitrile at $E_{app} = +0.63$ V, which transfers 1 electron per molecule of complex and leads to the generation of $\{Mn^{III}Cl_2(pypz-H)_2\}^+$ as attested by the CV obtained (Figure 2). However, the yield of Mn^{III} species is only 83% as judged by comparison between the intensities of the waves recorded before and after electrolysis, and two new irreversible oxidation waves appear at 0.8 and 1 V which, in the case of the latter, could tentatively be assigned to the oxidation of free chloride ions. The new wave at 0.8 V could be related to the presence of new Mn(II) species arising from substitution of Cl ligands by acetonitrile solvent, and the increase in the $E_{1/2}$ value with regard to the initial wave would be in accordance with the higher electron-withdrawing ability of CH_3CN when compared to chlorido.^{23,24} The cyclic voltammetry obtained after back-electrolysis performed at 0.3 V shows an increase of the intensity of the Mn^{III}/Mn^{II} redox wave but the initial species is not completely restored. The UV-Vis spectrum of the resulting oxidized compound was also performed (Figure S5) and shows the same features than other Mn^{III} complexes with nitrogen and chlorido based ligands described in the literature.^{23,25}

Catalytic olefin epoxidation in acetonitrile medium

The catalytic activity of manganese compounds **1-6** towards styrene epoxidation using peracetic acid (39%) as oxidant in acetonitrile was investigated. Table 1 reports the conversion and selectivity values for the epoxide product in each case. No epoxidation occurred in the absence of catalyst, and olefin conversion values were below 5% in the presence of different manganese salts. Hydrogen peroxide was also tested as oxidant but no catalytic activity was detected. Also, a combination of H_2O_2 (50% aqueous solution) and acetic acid at 0°C (1:10 H_2O_2 :AcOH ratio) was used but very low conversion values (<10%) were found.

As we can see in Table 1, all the compounds show moderate conversion and selectivity values for styrene epoxide and in all cases benzaldehyde (4-19% vs epoxide) is detected as main side product.²⁶ The conversion values displayed by chlorido precatalysts **1** and **5** are higher than those presented by the triflate (**2**), acetate (**3**) or nitrate (**4**) complexes. The differences observed can be explained by slower

oxidation kinetics for the latter three compounds since the oxidation potential of the chlorido complexes ($E_{1/2} = 0.63$ V, **1** and 0.66 V, **5**) are significantly lower than those of complexes **2-4** (above 0.7 V). Also, distinctive high-valent species are probably involved depending on the precatalyst used. In previous works^{8a} we have demonstrated the remarkable differences in the oxidised species formed from structurally analogous chlorido and triflate Mn complexes containing bipyridyl ligands, where the high-valent species formed by oxidation of the chlorido complexes attained a higher oxidation state thanks to the presence of Cl ligands that remained coordinated after addition of the oxidant, and this was related to the better catalytic performance observed for these complexes when compared to the analogous triflate compounds. A similar picture can be postulated for the epoxidation mediated by complexes **1-5**.

The activity of complex **6** is also moderate despite its pentacoordinated nature that in principle should favour the approach of the substrate towards the active site. This fact could be due to the strongly coordinating and electron-donor ability of the anionic phenolate moieties that would increase the stability of a putative high-valent metal-oxo intermediate hence decreasing its reactivity and leading to a lower conversion of substrate, as has been observed with other Mn(III) compounds.²⁶ In the case of complex **6**, we believe that the main factors affecting the reactivity are the nature of the ligands and the coordination environment rather than the oxidation state of the initial precatalyst.

In this context, we have also decided to study and compare the performances of compounds **1**, **6** and **5**, which present different number and types of bidentate ligands, coordination environments and Mn oxidation state, in the epoxidation of other olefins. Table 2 reports the conversion and the selectivity values obtained for the corresponding epoxide products.

As can be observed in Table 2, moderate conversion values are obtained in general for the three aromatic olefins tested (entries 1-3) whereas the three catalysts display better performances when epoxidizing the aliphatic cyclooctene and 4-vinylcyclohex-1-ene substrates (entries 4 and 5). Moderate to high selectivity values for the corresponding epoxides are observed in all cases, with formation of minor amounts of the corresponding aldehyde, alcohol or/and ketone.

The improved performance observed for the most electron-rich aliphatic substrates suggests that an electrophilic active species could be responsible for the attack at the alkene position. This is also in agreement with the catalysts leading specifically to the epoxidation of the ring alkene position at the 4-vinylcyclohex-1-ene substrate. The epoxidation of this olefin with manganese complexes has been only

scarcely studied²⁷ and the results indicate that either a mixture of the two possible regioisomers or the corresponding diepoxide are formed. To the best of our knowledge, the total epoxidation of the alkene ring position has never been reported with manganese compounds.

Concerning the epoxidation of the aromatic substrates (entries 1-3), it is interesting to observe the decrease of the conversion for compounds **1** and **5** with respect to compound **6** in the epoxidation of *cis* and *trans* β -methyl-styrene, which could be caused by the hexacoordinated nature of the former precatalysts that presumably leads to an increased steric encumbrance (the pyramidal complex **6** probably provides a faster route for the approach of the substrate). However, for styrene this behaviour is reversed thus indicating that, in this case, electronic factors dominate over the steric encumbrance and consequently complex **6**, containing the anionic *Ophpz-H* ligand, leads to a lower conversion degree. On the other hand, the epoxidation of the aliphatic substrates (entries 4 and 5) manifests both types of effects. Firstly, if we compare the two octahedral complexes **1** and **5**, the lower performance displayed by **5** is rather explained by electronic factors as a less electrophilic active species is expected for this catalyst that contains only one electron-acceptor *pypz-H* ligand, in contrast to the bis(*pypz-H*) complex **1**. On the contrary, the complete conversion attained by complex **6** evidences a structural influence since one would expect a poorly electrophilic intermediate for this catalyst containing two anionic *Ophpz-H* ligands, as discussed above for the aromatic substrates.

Regarding the oxidation of *cis*- β -methyl-styrene, the selectivity for the epoxide is high in all cases, but it is not stereospecific since 15% (for **1** and **6**) and 20% (for **5**) of *trans*-epoxide is produced. This behaviour is similar to that displayed by Mn(salen) catalysts bearing chlorido as counterion/axial ligand,²⁸ but it is different to [MnCl₂(L)₂], with L= bipyridylic ligands,^{5c,8a} where only *cis*-epoxide is produced. This result suggests in our compounds the presence of a long-lived free substrate radical during the oxygen transfer process^{7a} where the C-C bond rotation leading to *cis/trans* isomerization in the intermediate species formed is faster than the closure of the ring. It is surprising this variance in *cis/trans* selectivity when complex **1** is compared to the structurally analogous [MnCl₂(L)₂], where the only difference is the replacement of a pyridyl by a pyrazolyl ring in the bidentate ligand. It is clear that the pyrazole ring must have a distinctive electronic and/or structural influence in the stabilization of the intermediate species formed. The differences in the reaction pathway due to replacement of a pyridyl by a pyrazolyl ring have been analysed through DFT calculations (*vide infra*).

In order to obtain more information about the formation of high-valent species in acetonitrile after addition of peracetic acid, we carried out UV-vis spectroscopic measurements on compounds **1** and **6** with the idea to observe possible reactive intermediate species (see supporting information, Figures S6 and S7). In the case of complex **6** (Figure S6), when 2 eq. of peracetic acid were added to a solution containing the Mn(III) compound in acetonitrile at 25°C the initial dark green colour turned to greenish-brown, and the band at 636 nm was initially shifted to 680 nm. After 15 minutes, a decrease of the overall absorbance was observed. This latest spectrum can be attributed to a new Mn(III) species arising from oxidant and solvent coordination as evidenced by the ESI-MS spectrum of the solution (see below). At this point, styrene is added but no further changes are observed in the UV-vis spectra. Similar experiments (Figure S7) have been done with compound **1** at -10°C to slow the possible chemical transformations after addition of the oxidant (lowering the temperature to -10°C was not possible in the case of complex **6** because of its low solubility). The initial colourless solution of complex **1** changed to brown with the addition of peracetic acid and a new band appeared in the visible region at 570 nm with a strong increase of the absorbance below 490 nm. This band suggests the formation of Mn(III) species,²⁵ as also stated by the ESI-MS experiments described later. After 15 minutes the spectrum is unchanged in contrast with the behaviour displayed by complex **6**, indicating that low temperature is necessary to avoid degradation under these experimental conditions. In this case, subsequent addition of styrene (10 equivalents) induces a change in the spectrum, reducing this species to low-valent manganese (II) species. It must be noticed that the catalytic experiments previously described have been carried out at room temperature but using a large excess of oxidant, thus allowing the catalytic activity for both complexes.

Electrospray mass spectra were recorded in positive detection mode for both complexes after addition of peracetic (Figure S8). In the starting solution, ions at m/z 457.2 for **1** and 372.9 for **6** were detected, corresponding to $[\text{MnCl}_2(\text{pypz-H})_2]\text{H}_2\text{O}\cdot\text{Na}^+$ and $[\text{Mn}(\text{Ophpz-H})_2]^+$ respectively. After addition of peracetic at 0°C new peaks appear that, in the case of compound **1**, may be attributed to different cationic species of Mn(II), Mn(III) and oxo-bridged binuclear manganese (III) compounds. In the case of **6** only mononuclear cationic species of Mn(III) have been detected.

In addition to the species mentioned above, it should be noted that other high-valent mononuclear oxo or peroxy manganese species could be involved as catalytic active species, as has previously been reported in the epoxidation reaction with peracids.²⁹ Also, several types of reactive intermediates including *cis*- $\text{Mn}^{\text{IV}}(\text{O})_2$ and *trans*- $\text{Mn}^{\text{V}}(\text{O})_2$ ^{30,31} have been proposed in the literature for Mn-catalysed organic

oxidations. These intermediate species might be transiently formed upon addition of oxidant, but they are not spectroscopically observable, or they are present in a too low concentration to be detected in the experimental conditions tested.

Computational Results

DFT calculations have been carried out to unravel the origin of the about 15% of *cis*→*trans* isomerization in the epoxidation of the substrate *cis*-β-methyl styrene with Mn complex **1** in comparison with the total stereoselectivity for the *cis*-epoxide observed with [MnCl₂(L)] (L = SPAN ligands)^{5d} or [MnCl₂(L)₂](L = bipyridylic ligands).^{5c} Starting with the catalytic active species [Mn^{IV}(O)₂] generated from the precatalyst **1** we draw in Figure 3 the reaction profiles leading to *cis* and *trans* epoxides. The initial ground state of complex **1** is a doublet. Then it switches to quadruplet after the formation of the biradical species **II**. The reaction pathway follows the typical scheme for such epoxidations, with two steps that require overcoming low barriers for system **1**. Once the intermediate radical species **II**_{*cis*} is formed, the direct closure of the ring (**II**_{*cis*}→**III**_{*cis*}) requires overcoming a barrier of 2.0 kcal/mol, a value slightly higher than the 1.0 kcal/mol corresponding to the barrier of the *cis*→*trans* isomerization, **II**_{*cis*}→**II**_{*trans*}. However, the closure of the ring after isomerization through the subsequent transition state **II**_{*trans*}→**III**_{*trans*}, requires 0.6 kcal/mol more than the closing transition state **II**_{*cis*}→**III**_{*cis*} leading to *cis* epoxide. This explains why there is some degree of *cis*→*trans* isomerization although at the end the *cis* epoxidized product is the main product obtained experimentally despite being 1.1 kcal/mol less stable.

As discussed before, the stereoselectivity observed in catalyst **1** is different to that found in catalysts with non-pyrazolic based ligands. To explore the origin of this difference we have calculated the reaction mechanism in some non-pyrazolic based ligands (complexes **8** and **9**, Figure S9). In addition, in complex **7** we have substituted the NH groups of catalyst **1** by CH₂, to discuss the role of H-bonds due to the NH groups. In all cases, the reaction profile is quite similar (see Table 3), although some differences are observed. If we focus the discussion on the stereoselectivity of the reaction, we have to analyze the reaction pathways starting from **II**_{*cis*}. For complex **7** the energy barriers of the reactions **II**_{*cis*}→**III**_{*cis*} and **II**_{*cis*}→**II**_{*trans*} are very low, 0.5 and 0.3 kcal/mol respectively. On the other hand, the **II**_{*trans*}→**III**_{*trans*} process has to surpass a barrier of 3.2 kcal/mol. Overall, for **7**, application of the Curtin-Hammett principle leads to the conclusion that the *cis* product formation will be favored in this case. To compare the role of pyridyl and pyrazole based ligands, we envisaged calculations with complexes **8** and **9**, which

experimentally have demonstrated to give selective *cis* epoxidation from *cis* substrates. Bearing in mind the previously reported SPAN based system **8** (see Figure S9),^{5d} we found a relative instability of the **II_{cis}** species that would not favor the *cis*→*trans* isomerization but the direct closure of the *cis* epoxide ring through a barrierless step (**II_{cis}**→**III_{cis}**), i.e., the key results to point out are that the barrier of the isomerization **II_{cis}**-**II_{trans}** is 2.0 kcal/mol higher in energy than the closure of the *cis* epoxide, exactly the opposite with respect to the situation found in **1**. Consequently, for catalyst **8**, **II_{trans}** is not formed and the reaction is completely stereoselective. To find a reason for the higher reactivity of **8** as compared to **1** in the **II_{cis}**→**III_{cis}** process, we looked at the NBO charges of intermediate **II_{cis}** and we found only slight differences. For instance, the negative charge of the oxygen atom attacking the C atom to close the ring is 0.03 electrons more negative in **8**. Even though this slightly different charge can make a difference, we think that the main reason for the larger reactivity of the **II_{cis}**→**III_{cis}** process in **8** has to be ascribed to the different O...C distance in the **II_{cis}** that will be transformed into a O-C bond in **III_{cis}**. This distance is nearly 0.3 Å shorter for complex **8** (see Figure S10), with respect to complex **1**.

On the other hand, the use of a bipyridyl ligand in **9** instead of five-membered rings like in systems **1** and **7** (see Figure S9), and with added sterical hindrance due to the presence of a pinene group in each bipyridine, confirms that the formation of *trans* epoxides was not possible because **II_{cis}**-**II_{trans}** transition state is 3.1 kcal/mol higher in energy with respect to the closure of the *cis* epoxide through the **II_{cis}**-**III_{cis}** pathway and thus, no competition is likely.

Further calculations on the epoxidation of the 4-vinylcyclohex-1-ene substrate by **1**-[Mn^{IV}(O)₂] confirmed the experimentally found complete selectivity towards the alkene epoxidation at the ring position. Indeed, the first barrier of the reaction pathway, which would be equivalent to the **I_{cis}**-**II_{cis}** step displayed in Figure 3 for the *cis*-β-methylstyrene substrate, is located 1.8 kcal/mol higher in energy for the terminal epoxidation than for the ring epoxidation.

Catalytic olefin epoxidation in different media. Reusability of catalysts in ionic liquid:CH₃CN.

We have also tested the performance of precatalysts **1**, **5** and **6** in media different to the above described acetonitrile. Current research has been going on in trying to find new solvents with a small environmental impact.¹¹ The need to develop sustainable oxidation processes lead us to test the effect of different clean solvents as ionic liquids or glycerol on the epoxidation of alkenes using compounds **1**, **5** and **6** as catalysts, and the results obtained are shown in Table 4. As was the case for the catalytic experiments

performed in acetonitrile, no epoxidation occurred in the absence of catalyst or in the presence of Mn salts, in the different media studied. The substrates chosen for this study were *cis* and *trans*- β -methylstyrene and cyclooctene, and the ionic liquid (IL) used was the commercially available [bmim]PF₆.

~~We have investigated~~ The catalytic performance of these compounds ~~in~~ when using ionic liquid media was first investigated using different IL:acetonitrile ratios. Without acetonitrile solvent (see for instance entry 5 in Table 4), we obtained high conversions but low selectivity values, presumably due to the hydrolysis and/or overoxidation of the corresponding epoxide.³² In general, better conversion values are obtained in presence of IL:CH₃CN 1:1 ([bmim]PF₆:acetonitrile ratios from 1:0 to 1:1 were tested, see SI). The selectivity for the epoxide product is well maintained in IL:CH₃CN 1:1 mixture when compared to acetonitrile with only a slight decrease in some cases, but it is important to note that the presence of the ionic liquid exerts a significant stabilizing effect on our catalysts, and the conversions are improved particularly for complex **1** (compare entries 1 and 2, or 4 and 6) and are well maintained at moderate to high values for the case of complexes **5** and **6**. The ionic liquids have been described to have a variety of distinctive effects in catalysis (being in some cases directly involved in the catalytic path) and, in our case, we can postulate a stabilizing effect arising from electrostatic or π -cation interactions between the bmim⁺ cation and the aromatic rings of the ligands in the intermediate Mn species.³³ However, the presence of acetonitrile is essential to achieve good selectivities for the epoxide product, and a possible reason is that it could inhibit the mechanism of hydrolysis in a similar way to other coordinating base species which block the access of the epoxide to the acidic metal centre inhibiting the hydrolysis and consequently increasing the selectivity for the corresponding epoxide.³⁴

The reaction in glycerol leads to an increase in the conversion values for the methylstyrene substrates (compare entries 1 and 3, or 4 and 7) but in the case of cyclooctene only a moderate conversion is attained. Also, the selectivity values for the corresponding epoxides are moderate, probably due to the hydrolysis of the epoxide as described previously for the IL:acetonitrile systems.¹³ In the case of cyclooctene the selectivity values in glycerol are higher than for the two methylstyrene substrates but, although a decrease in the selectivity was observed for the latter, a total stereospecificity was observed for the *cis* epoxide in the epoxidation of *cis*- β -methylstyrene mediated by the complexes synthesized. In this context, these preliminary results are promising for the use of glycerol as a green solvent in oxidation processes using peracetic acid as oxidant. As we have previously reported, the performance of compound

1 as catalyst in these media is better than ~~the one that~~ displayed by compound **5**, which corroborates again the role of pyrazolic ligands in the modulation of the catalytic activity.

Based in the above results, the recyclability of the catalytic systems **1** and **6** was investigated in [bmim]PF₆:CH₃CN medium and the results obtained for both catalysts are displayed in Figure 4 and in Figures S11 and S12. One can observe that the catalysts maintain an excellent performance through up to 12 runs in all cases. The selectivity towards the epoxide product is also well maintained and the conversion values are near 100% for *trans*- β -methylstyrene (Figure 4) and cyclooctene (Figure S12), and close to 90% for *cis*- β -methylstyrene (Figure S11). In this latest case, the selectivity for the *cis* epoxide is maintained through all the runs and this value is higher than in acetonitrile solvent (< 5% of *trans* epoxide isomer has been obtained for catalyst **1** and < 10% for catalyst **6**, whereas in acetonitrile this value was around 15%). The overall turnover numbers for the obtaining of the respective epoxides are 914 (complex **1**) / 1033 (complex **6**) for *trans*- β -methylstyrene, 1190 (complex **1**) for cyclooctene and 915 (complex **1**) / 880 (complex **6**) for *cis*- β -methylstyrene. It is worth to notice the good stabilizing effect of ionic liquid on the catalysts that allows their reuse without loss of activity and keeping excellent selectivity values.

To the best of our knowledge, these systems constitute one of the most effective and stable epoxidation systems based on the reutilization of manganese compounds and the first example of Mn(II) and Mn(III) complexes with pyrazole- based ligands tested under such conditions.

Conclusions

We have synthesized and fully characterized a family of new Mn(II) and Mn(III) complexes containing pyrazole-based ligands. The X-ray structures for complexes **1-4**, bearing *pypz-H* ligands, display hexacoordinated Mn(II) ions obtaining in all the cases the Δ/Λ *cis-X-trans-pz* isomer, which seems to be energetically favoured thanks to H-bonding interactions involving the pyrazolic H atoms and the monodentate ligands. Complex **6** contains the *Ophpz-H* and monodentate chlorido ligands, it displays a penta-coordinated Mn(III) environment and has been also obtained as a single isomer. Complex **5** is the first co-crystal of Mn(II) that contains two isomers, *trans*-Cl-*cis*-H₂O and *cis*-Cl-*trans*-H₂O.

All complexes have been studied as precatalysts in the epoxidation of styrene using peracetic acid as oxidant. Among the structurally analogous six-coordinated complexes **1-4**, the increased performance by chlorido with respect to triflate, acetate and nitrate complexes reveals the role of the monodentate ligands

in the catalytic activity observed. Chlorido complexes **1**, **5** and **6** have proven to be active in the epoxidation of other alkenes in acetonitrile. In the case of cyclooctene and 4-vinylcyclohex-1-ene substrates high conversions and good selectivity values have been achieved with these complexes, being the first reported that epoxidize specifically the ring alkene of 4-vinylcyclohex-1-ene. The epoxidation of *cis*- β -methylstyrene mediated by the three catalysts shows moderate to high selectivity for the epoxide, but the stereospecificity is not complete for the formation of the *cis* epoxide, displaying a certain degree of *cis* to *trans* isomerization. This result is in agreement with the computational calculations performed on complex **1**, which predict a lower barrier for the closure of the *cis* epoxide than for the isomerization step, but where the overall energy difference of only 0.6 kcal/mol explains the partial formation of the thermodynamically more stable *trans* epoxide. Further studies with other catalysts bearing 5- and 6-membered rings bonded to the metal have demonstrated that the pyrazole rings have a key role to explain the lack of stereoselectivity in **1**.

In general, conversion and selectivity values for the epoxidation mediated by compound **1** (containing two pyrazolic ligands coordinated to Mn(II)) have been found to be higher than those presented by compound **5** (containing only one pyrazolic ligand). These results highlight the crucial role that pyrazolic ligands seem to have in the fine tuning of the intermediated species formed during oxidative catalysis. On the other hand, both electronic and structural factors seem to play a role in the performance exhibited by the pentacoordinated precatalyst **6**, though the metal oxidation state seems not to be relevant.

Mn chlorido complexes have also been investigated in epoxidation catalysis carried out in other media such as glycerol, a solvent with promising preliminary results for its use as ~~a~~-green solvent in oxidation processes using peracetic acid as oxidant. The epoxidation in an ionic liquid:solvent medium shows a remarkable effectiveness and selectivity for the epoxide product. Also, an excellent degree of reusability in the epoxidation of some alkenes in this medium has been observed for catalysts **1** and **6** which were found to be robust and recyclable catalytic systems that can be reused without loss of activity and keeping high conversion and selectivity values after twelve cycles.

Experimental

Materials

All reagents used in the present work were obtained from Aldrich Chemical Co and were used without further purification. Reagent grade organic solvents were obtained from SDS and high purity de-ionized water was obtained by passing distilled water through a nano-pure Mili-Q water purification system.

Instrumentation and measurements.

FT-IR spectra were taken in a Mattson-Galaxy Satellite FT-IR spectrophotometer containing a MKII Golden Gate Single Reflection ATR System. UV-Vis spectroscopy was performed on a Cary 50 Scan (Varian) UV-Vis spectrophotometer with 1 cm quartz cells. Cyclic voltammetric (CV) and differential pulse voltammetry (DPV) experiments were performed in a IJ-Cambria IH-660 potentiostat using a three electrode cell. Glassy carbon electrodes (3 mm diameter) from BAS were used as working electrode, platinum wire as auxiliary and Ag/AgNO₃ as the reference electrode. All cyclic voltammograms presented in this work were recorded under nitrogen atmosphere at a scan rate of 100 mV/s. The $E_{1/2}$ values were estimated from cyclic voltammetry as the average of the oxidative and reductive peak potentials $(E_{pa}+E_{pc})/2$ or directly from DPV. Unless explicitly mentioned the concentration of the complexes were approximately 1 mM. Elemental analyses were performed using a CHNS-O Elemental Analyser EA-1108 from Fisons. ESI-MS experiments were performed on a Navigator LC/MS chromatograph from Thermo Quest Finnigan, using acetonitrile as a mobile phase. ¹H NMR spectra were recorded on a Bruker DPX400 Model Advance (4.7) (400 MHz) instrument. Chemical shifts are reported in δ (parts per million) relative to an internal standard (tetramethylsilane).

X-ray structure determination.

Measurement of the crystals were performed on a Bruker Smart Apex CCD diffractometer using graphite-monochromated Mo K α radiation ($\lambda = 0.71073\text{\AA}$) from an X-Ray tube. Data collection, Smart V. 5.631 (Bruker AXS 1997-02); data reduction, Saint+ Version 6.36A (Bruker AXS 2001); absorption correction, SADABS version 2.10 (Bruker AXS 2001) and structure solution and refinement, structure solution and refinement, SHELXL-2013 (Sheldrick, 2013). The crystallographic data as well as details of the structure solution and refinement procedures are reported in supporting information. CCDC 1031995 (1), 1031996 (2), 1031997 (3), 1032000(4), 1031998 (5), 1031999 (6) contain the supplementary crystallographic data

for this paper. These data can be obtained free of charge from The Cambridge Crystallographic Data Centre via www.ccdc.cam.ac.uk/products/csd/request/

Preparations

The (2-(3-pyrazolyl)pyridine)³⁵ ligand (*pypz-H*) and Mn(CF₃SO₃)₂³⁶ were prepared according to literature procedures. All synthetic manipulations were routinely performed under ambient conditions.

Synthesis of HO ϕ p ϕ z-H ligand

The ligand HO ϕ p ϕ z-H was prepared following a different method to that described in the literature.³⁷

3(5)-(2'-hydroxyphenyl)pyrazole (HO ϕ p ϕ z-H): 5 g (36.7 mmol) of 2'-hydroxyacetophenone and 7 mL (52.6 mmol) of N,N-dimethylformamide dimethylacetal were introduced in a round-bottomed flask. The reaction mixture was refluxed overnight at 160 °C. A solid, corresponding to 3-(dimethylamino)-1-(1-hydroxyphen-2-yl)prop-2-en-1-one, **L**, precipitated after cooling to room temperature. That solid was collected by filtration, washed with hexane (3 x 100 mL) and diethyl ether (3 x 100 mL), and dried at vacuum. Yield 5.05 g (72 %). ¹H NMR (400 MHz, CDCl₃, 20°C): δ = 2.97 (s, 3 H, CH₃), 3.19 (s, 3 H, CH₃), 5.78 (d, ³J_{H,H} = 16 Hz, 1 H, H_e), 6.81 (t, ³J_{H,H} = 10.8 Hz, 1 H, H_c), 6.93 (d, ³J_{H,H} = 11.2 Hz, 1 H, H_a), 7.34 (t, ³J_{H,H} = 11.2 Hz, 1 H, H_b), 7.69 (d, ³J_{H,H} = 10.8 Hz, 1 H, H_d), 7.88 (d, ³J_{H,H} = 16 Hz, 1 H, H_f), 13.92 (s, 1 H, OH) ppm. In a second step, 2.76 g (14.43 mmol) of **L** in ethanol (9 mL) and 6 mL (123.5 mmol) of hydrazine were introduced in a round-bottomed flask. The mixture was heated at 60 °C and stirred for 30 min at this temperature. After reducing the volume and cooling to room temperature, 30 mL of distilled water were added, giving rise to the precipitation of a brown solid corresponding to HO ϕ p ϕ z-H ligand. This solid was filtered off, washed with hexane (2 x 200 mL) and dried at 100 °C for 1 h. After cooling, the product was recrystallized in ethanol (5 mL), obtaining a pale brown powder. Yield 1.31 g (57 %). ¹H NMR (400 MHz, CDCl₃, 20°C): δ = 6.73 (d, ³J_{H,H} = 3.4 Hz, 1 H, H_d), 6.93 (ddd, ³J_{H,H} = 10.3, 9.7 Hz, ⁴J_{H,H} = 1.2 Hz, 1 H, H_c), 7.04 (dd, ³J_{H,H} = 10.9 Hz, ⁴J_{H,H} = 1.6 Hz, 1 H, H_a), 7.24 (ddd, ³J_{H,H} = 10.9, 9.7 Hz, ⁴J_{H,H} = 2.2 Hz, 1 H, H_b), 7.61 (dd, ³J_{H,H} = 10.3 Hz, ⁴J_{H,H} = 2.2 Hz, 1 H, H_d), 7.63 (d, ³J_{H,H} = 3.4 Hz, 1 H, H_f) ppm.

Synthesis of manganese complexes

Preparation of [MnCl₂(*pypz-H*)₂] \cdot H₂O (1**):** A solution of *pypz-H* (0.144 g, 0.992 mmol) and 0.049 g (0.389 mmol) of MnCl₂ in ethanol (5 mL) was stirred for 30 min at room temperature. A pale yellow precipitate was obtained that was collected by filtration, washed thoroughly with diethyl ether and dried in air. The resulting pale yellow solution was left to evaporate at room temperature. After one week, air-

stable, colorless crystals of **1**, suitable for X-ray diffraction analysis, were obtained. Yield: 0.15 g (94 %). Anal. Found (Calc.) for $C_{16}H_{14}N_6Cl_2Mn \cdot H_2O$: C, 44.07 (44.26); H, 3.1 (3.71); N, 19.17 (19.36) %. IR (cm^{-1}): $\nu = 3106-3045$ (ν (NH)); 1600 (ν (C-N) sp^2); 1433 (ν (C-C) sp^2) cm^{-1} . $E_{1/2}$ (III/II): 0.63 V vs. Ag/AgNO₃ (CH₃CN + 0.1M [(nBu)₄N]PF₆). ESI-MS (m/z): 457 ([MnCl₂(pypz-H)₂] \cdot H₂O)Na⁺.

Preparation of [Mn(CF₃SO₃)₂(pypz-H)₂] (2): A solution of *pypz-H* (0.115 g, 0.792 mmol) and Mn(CF₃SO₃)₂ (0.141 g, 0.399 mmol) in THF (5 mL) was stirred for one hour at room temperature. Afterwards, the volume of the solution was reduced to 1 mL and a pale yellow precipitate was obtained. This solid was filtered off, washed thoroughly with diethyl ether and dried in air. After two days, air-stable, colorless crystals, suitable for X-ray diffraction analysis, were obtained. Yield: 0.24 g (93.5 %). Anal. Found (Calc.) for $C_{18}H_{14}N_6S_2O_6F_6Mn$: C, 33.54 (33.60); H, 2.32 (2.19); N, 13.65 (13.06) %. IR (cm^{-1}): $\nu = 3238-3142$ (ν (N-H)); 1607 (ν (C-N) sp^2); 1434 (ν (C-C) sp^2); 1223-1172 (ν (S-O) sp^2). cm^{-1} . $E_{1/2}$ (III/II): 0.72 V vs. Ag/AgNO₃ (CH₃CN + 0.1M [(nBu)₄N]PF₆). ESI-MS (m/z): 494 [Mn(CF₃SO₃)(pypz-H)₂]⁺.

Preparation of [Mn(OAc)₂(pypz-H)₂] \cdot H₂O (3): 0.107 g (0.737 mmol) of *pypz-H* were added under stirring to a solution of Mn(OAc)₂ \cdot 4H₂O (0.086 g, 0.356 mmol) in acetonitrile (5 mL). A pale yellow product was obtained after one hour. This solid was collected by filtration, washed thoroughly with diethyl ether and dried in air. By recrystallization of the product in CH₂Cl₂, colorless plates of **3** suitable for X-ray diffraction were obtained. Yield: 92.4 mg (57 %). Anal. Found (Calc.) for $C_{20}H_{22}N_6O_5Mn$: C, 49.57 (49.90); H, 4.01 (4.60); N, 17.52 (17.45) %. IR (cm^{-1}): $\nu = 3145-3050$ (ν (NH)); 2926 (ν (C-H) sp^3); 1587 (ν (COO⁻)_{as}); 1407 (ν (COO⁻)_s); 899 (δ (COO⁻)) cm^{-1} . $E_{1/2}$ (III/II): 0.74 V vs. Ag/AgNO₃ (CH₃CN + 0.1M [(nBu)₄N]PF₆). ESI-MS (m/z): 558 [{Mn(pypzH)}₂(μ -OAc)₃]⁺.

Preparation of [Mn(NO₃)₂(pypz-H)₂] (4): 0.15 g (1 mmol) of *pypz-H* were added to a solution of Mn(NO₃)₂ \cdot 4H₂O (0.13 g, 0.5 mmol) in ethanol (5 mL) under stirring. After one hour, diethyl ether was added, giving rise to the precipitation of a pale brown solid that was collected by filtration, washed thoroughly with diethyl ether and dried in air. Suitable crystals as colorless blocks were grown by diffusion of ethyl ether into an acetone solution of the compound. Yield: 0.18 g (74%). Anal. Found (Calc.) for $C_{16}H_{14}N_8O_6Mn$: C, 39.39 (40.95); H, 2.96 (3.01); N, 22.86 (23.88) %. IR (cm^{-1}): $\nu = 3174$ (ν (OH)); 3045-2925 (ν (NH)); 1607-1517 (ν (NO₂)); 1431 (ν (C-C) sp^2); 1301 (ν (C-N) sp^2). E_{pa} (III/II): 0.73 V vs. Ag/AgNO₃ (CH₃CN + 0.1M [(nBu)₄N]PF₆). ESI-MS (m/z): 489 ([Mn(NO₃)₂(pypz-H)₂] \cdot H₃O⁺).

Preparation of [MnCl₂(pypz-H)(H₂O)₂] (5): To a solution of MnCl₂ (0.087 g, 0.695 mmol) in ethanol (5 mL), 0.102 g of *pypz-H* (0.705 mmol) were added under stirring. The resulting pale yellow solution was stirred for 10 min and afterwards a white solid precipitated. This solid was filtered off, washed with diethyl ether and dried in air. Colorless plates, suitable for X-ray diffraction, were grown by recrystallization in ethanol. Yield: 0.16 g (73 %). Anal. Found (Calc.) for C₈H₁₁Cl₂Mn N₃O₂: C, 31.47 (31.29); H, 3.55 (3.61); N, 13.73 (13.69) %. IR (cm⁻¹): $\nu = 3328-3222$ (ν (OH)); 3140-3119 (ν (NH)); 1606 (ν (C-N)_{sp²}); 1429 (ν (C-C)_{sp²}) cm⁻¹. $E_{1/2}$ (III/II): 0.66 V vs. Ag/AgNO₃ (CH₃CN + 0.1M [(nBu)₄N]PF₆). ESI-MS (m/z): 660 [{MnCl(H₂O)(pypzH)}₂(μ -Cl)₂] \cdot Na⁺.

Preparation of [MnCl(Ophpz-H)₂] \cdot 3H₂O (6): 100 mg (0.624 mmol) of *HOpzp-H* were added to a solution of MnCl₂ (39.3 mg, 0.312 mmol) in ethanol (5 mL) under stirring. Afterwards, 0.3 mL of NaOH 1M were added to the reaction mixture and this solution turned from yellow to dark green. After one hour, 15 mL of distilled water were added, giving rise to the precipitation of a dark green solid that was collected by filtration, washed thoroughly with cool water and dried in air. After one week, air-stable, dark green crystals of **6**, suitable for X-ray diffraction analysis, were obtained from the mother liquor. Yield: 27.6 mg (19 %). Anal. Found (Calc.) for C₁₈H₁₄ClN₄O₂Mn \cdot 3H₂O: C, 46.74 (46.71); H, 4.10(4.36); N, 12.05 (12.10) %. IR (cm⁻¹): $\nu = 3360-3258$ (ν (OH)); 1601-1560 (ν (C-N)_{sp²}). $E_{p,a}$ (IV/III): 0.63 V vs. Ag/AgNO₃ (CH₃CN + 0.1M [(nBu)₄N]PF₆). UV-Vis (CH₃CN): λ_{max} , nm (ϵ , M⁻¹ cm⁻¹) 636 (202.34). ESI-MS (m/z) 373 [Mn(Ophpz-H)₂]⁺.

Catalytic epoxidation.

An anhydrous CH₃CN (1 mL) solution of alkene (250 μ mol), catalyst (2.5 μ mol) and biphenyl (250 μ mol, internal standard) was prepared in a 5 mL flask and cooled in an ice bath. At this point, 39 % peracetic acid (500 μ mol) was added via syringe over 3 minutes under stirring. The reaction vessel was then taken out of the ice bath and allowed to progressively warm to RT. Each aliquot of the reaction taken for analysis was filtered through a basic alumina plug and was analyzed in a Shimadzu GC-2010 gas chromatography apparatus equipped with an Astec CHIRALDEX G-TA column and a FID detector, and quantification was achieved from calibration curves.

Catalytic epoxidation in ionic liquid:solvent media.

Catalyst (2.5 μ mol) and substrate (250 μ mol) were dissolved in 2 mL of [bmim]PF₆:CH₃CN (1:1) (bmim = 1-butyl-3-methylimidazolium). 39% peracetic acid (500 μ mol) was added via syringe over 3 minutes at

0°C. Afterward the solution was stirred at room temperature for 3 h. After completion, CH₃CN was removed under vacuum and the resulting suspension was washed with diethylether (3x5 mL) to extract the epoxide (which is then analyzed by GC after addition of 250 μmol of biphenyl) and the oxidant by-products. The remaining mixture was washed with NaOH aqueous solution and dried in vacuo. A new load of substrate and oxidant dissolved in acetonitrile was then added and the mixture was left for an additional 3 h run. This procedure was repeated up to twelve times.

Computational details

The density functional calculations were performed at the GGA level with the Gaussian09 set of programs,³⁸ with the M06L correlation-exchange functional.³⁹ The electronic configuration of the molecular systems was described by the standard SVP basis set, i.e. the split-valence basis set with polarization functions of Ahlrichs and co-workers, for H, C, N, and O.⁴⁰ For Mn we used the small-core, quasi-relativistic Stuttgart/Dresden effective core potential (standard SDD basis set in Gaussian09) basis set, with an associated valence basis set.⁴¹ All open-shell species were treated using the unrestricted formalism.

The geometry optimizations were performed without symmetry constraints, and the nature of the extrema was checked by analytical frequency calculations. Furthermore, connections between minima and transition states were confirmed by calculation of the intrinsic reaction paths. The Gibbs energies discussed throughout the text contain thermal and ZPE corrections. Solvent effects have been estimated in single point calculations on the gas phase optimized structures with triple zeta valence plus polarization (TZVP keyword in Gaussian) using the M06L functional,³⁷ however estimating solvent effects with the polarizable continuous solvation model PCM using acetonitrile as solvent.⁴² Therefore, all reported Gibbs energies are M06/SVP~SDD electronic energies with added thermal, ZPE, and solvent corrections obtained at the same M06/SVP~SDD level of theory.

Acknowledgements

This research has been financed by MINECO of Spain through projects, CTQ2010-21532-C02-01 and CTQ201123156/BQU. EM thanks UdG for a predoctoral grant. Serveis Tècnics de Recerca (STR) from UdG are also acknowledged for technical support. AP thanks the Spanish MINECO for a Ramón y Cajal contract (RYC-2009-05226) and European Commission for a Career Integration Grant (CIG09-GA-2011-

293900). MS thanks EU for a FEDER fund (UNGI08-4E-003) and the Generalitat de Catalunya for project 2014SGR931 and ICREA Academia 2009 prize.

Scheme 1. Synthetic strategy for the synthesis of complexes **1-6**.

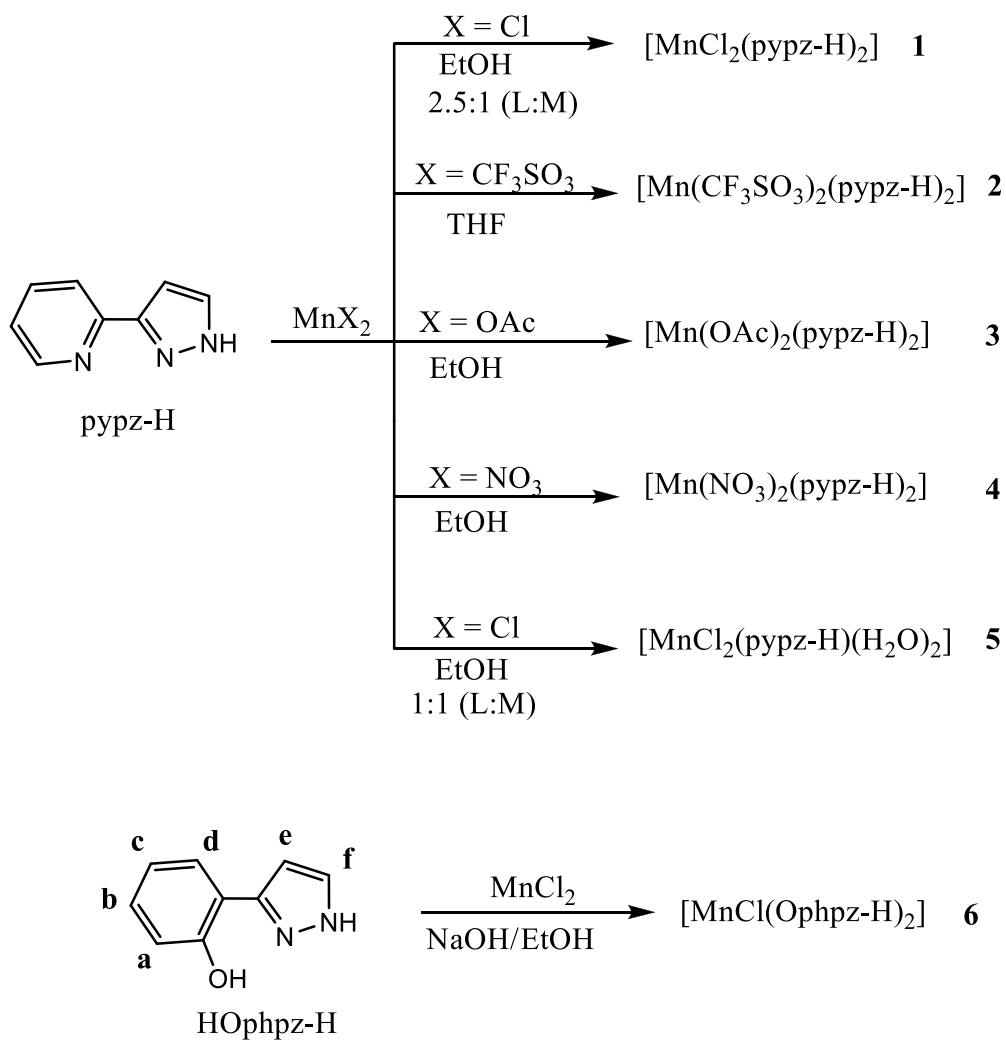
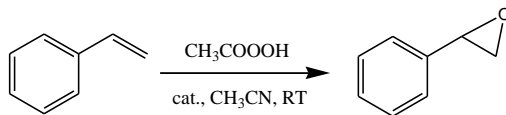


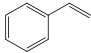
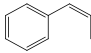
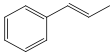
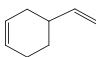
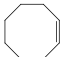
Table 1. Catalytic oxidation of styrene by Mn complexes **1-6** using peracetic acid as oxidant.^a Conversion (conv) and selectivity (sel) values are given in %.



Entry	compound	conv	sel ^b
1	[MnCl ₂ (pypz-H) ₂], 1	47	60
2	[Mn(CF ₃ SO ₃) ₂ (pypz-H) ₂], 2	22	30
3	[Mn(CH ₃ CO ₂) ₂ (pypz-H) ₂], 3	26	55
4	[Mn(NO ₃) ₂ (pypz-H) ₂], 4	24	61
5	[MnCl ₂ (pypz-H)(H ₂ O) ₂], 5	51	47
6	[MnCl(Ophpz-H) ₂], 6	34	50

^aConditions: catalyst (2.5 μmol), substrate (250 μmol), CH₃CN (1 mL). Peracetic acid 39% (500 μmol) added in 3 minutes at 0°C, then 3 hours of reaction at RT. ^bSelectivity for epoxide (sel): [Yield/Conversion]x100.

Table 2. Catalytic epoxidation of different alkenes with compounds **1**, **5** and **6** using peracetic acid as oxidant.^a Conversion (conv) and selectivity (sel) values are given in %.

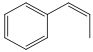
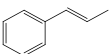
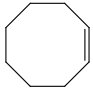
Entry	Substrate	[MnCl ₂ (pypz-H) ₂], 1		[MnCl ₂ (H ₂ O) ₂ (pypz-H)], 5		[MnCl(Ophpz-H) ₂], 6	
		conv	sel ^b	conv	sel	conv	sel
1		47	60	51	47	34	50
2		41	89 ^c	33 ^c	68 ^c	61	84 ^c
3		61	>99	47	58	87	85
4		>99	92 (100/0) ^d	80	90 (100/0) ^d	>99	63 (100/0)
5		>99	>99	86	>99	98	>99

^aConditions: catalyst (2.5 μmol), substrate (250 μmol), CH₃CN (1 mL). Peracetic acid 39% (500 μmol) added in 3 minutes at 0°C, then 3 hours of reaction at RT. ^bSelectivity for epoxide (sel): [Yield/Conversion]x100. ^c15% of *trans* epoxide isomer has been obtained for catalysts **1** and **6** whereas it was of 20% for **5**. ^dRatio [ring epoxide/vinyl epoxide]

Table 3. Reaction coordinate energies (in kcal/mol) for epoxidation of the *cis*- β -methylstyrene substrate with catalysts **1**, **7**, **8**, and **9**.

Cat	[Mn ^{IV} O ₂]	I _{cis}	I _{cis} -II _{cis}	II _{cis}	II _{cis} -III _{cis}	III _{cis}	II _{cis} -II _{trans}	II _{trans}	II _{trans} -III _{trans}	III _{trans}
1	39.8	32.4	32.5	7.7	9.7	0.0	8.7	7.7	10.3	-1.1
7	35.6	30.6	33.9	9.2	9.7	0.0	9.5	8.0	11.2	-2.5
8	33.4	31.3	32.0	7.5	8.8	0.0	10.8	5.6	6.9	-1.0
9	37.8	31.5	32.2	8.4	10.1	0.0	13.2	6.9	7.0	-2.8

Table 4. Epoxidation tests performed with complexes **1**, **5** and **6** in different media.^a Conversion (conv) and selectivity (sel) values are given in %.

Substrate	Solvent	[MnCl ₂ (pypz-H) ₂], 1		[MnCl ₂ (H ₂ O) ₂ (pypz-H)], 5		[MnCl(Ophpz-H) ₂], 6		Entry
		conv	sel ^b	conv	sel	conv	sel	
	CH ₃ CN	41	89 ^c	33	68 ^c	61	84 ^c	1
	[bmim]PF ₆ :CH ₃ CN	80	80 ^d	43	70 ^d	65	80 ^d	2
	glycerol	73	57 ^e	38	32 ^e	76	25 ^e	3
	CH ₃ CN	61	>99	47	58	87	85	4
	[bmim]PF ₆	99	<10	76	14	97	<10	5
	[bmim]PF ₆ :CH ₃ CN	85	96	54	83	82	97	6
	glycerol	86	38	71	20	90	17	7
	CH ₃ CN	>99	>99	86	>99	98	99	8
	[bmim]PF ₆ :CH ₃ CN	>99	>99	73	>99	99	97	9
	glycerol	64	76	69	69	74	98	10

^aConditions: catalyst (2.5 μmol), substrate (250 μmol), solvent (2 mL). Peracetic acid 39% (500 μmol) added in 3 minutes at 0°C, then 3 hours of reaction at RT. ^bSelectivity for epoxide (sel): [Yield/Conversion]x100. ^c15% of *trans* epoxide isomer has been obtained for catalysts **1** and **6** whereas it was of 20% for **5**. ^d< 5% of *trans* epoxide isomer has been obtained for both catalysts. ^e 100% of *cis* epoxide has been obtained.

Figure Captions

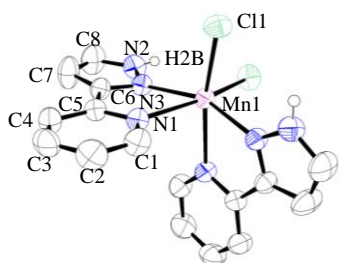
Figure 1. Ortep plots and labelling schemes for compounds **1-6**.

Figure 2. CV of a 1 mM acetonitrile solution containing 0.1 M *n*-Bu₄NPF₆ (TBAH) of **1** a) before electrolysis, b) and c) after electrolysis at 0.63V, d) after back-electrolysis at 0.3V. The initial scan direction is indicated by arrows in all cases.

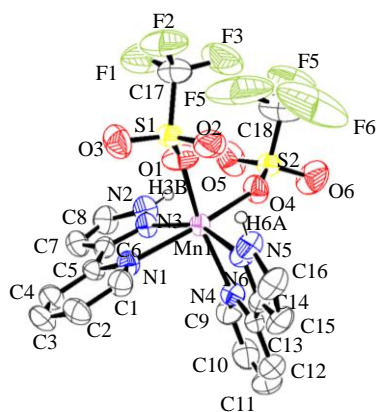
Figure 3. Reaction pathway for the epoxidation of the *cis*- β -methylstyrene substrate by the catalyst **1** (Gibbs energies in kcal/mol).

Figure 4. Conversion (black bars) and selectivity (grey bars) values obtained throughout a number of consecutive reuses of complex **1** (a) and **6** (b) in the epoxidation of *trans*- β -methylstyrene in [bmim]PF₆:CH₃CN.

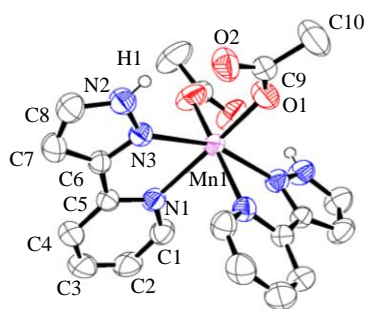
Figure 1.



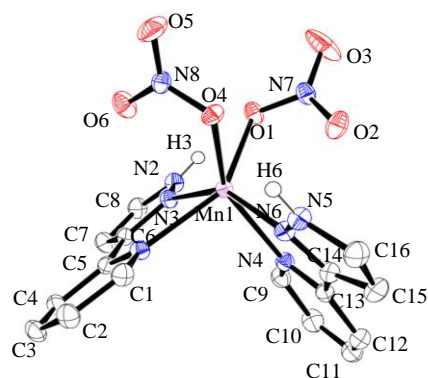
1



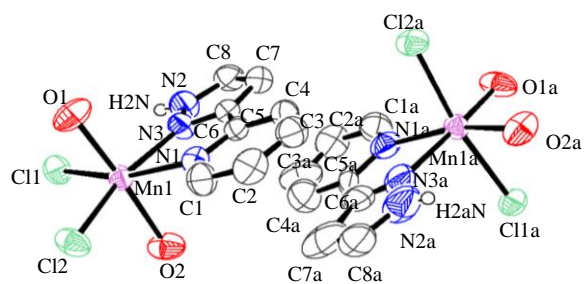
2



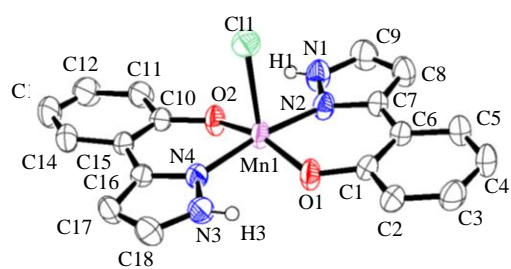
3



4



5



6

Figure 2.

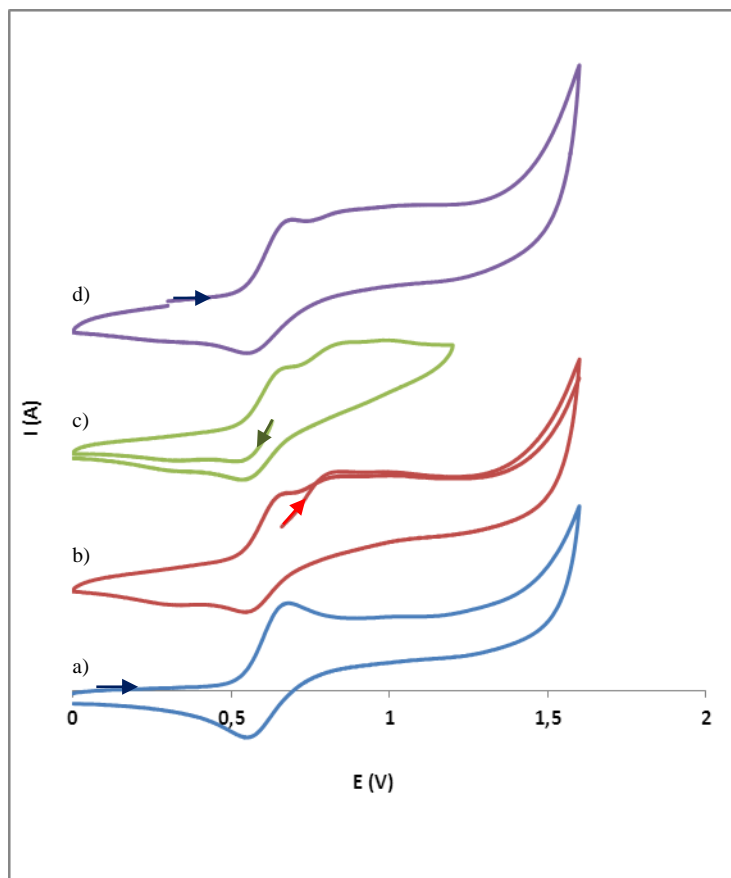


Figure 3.

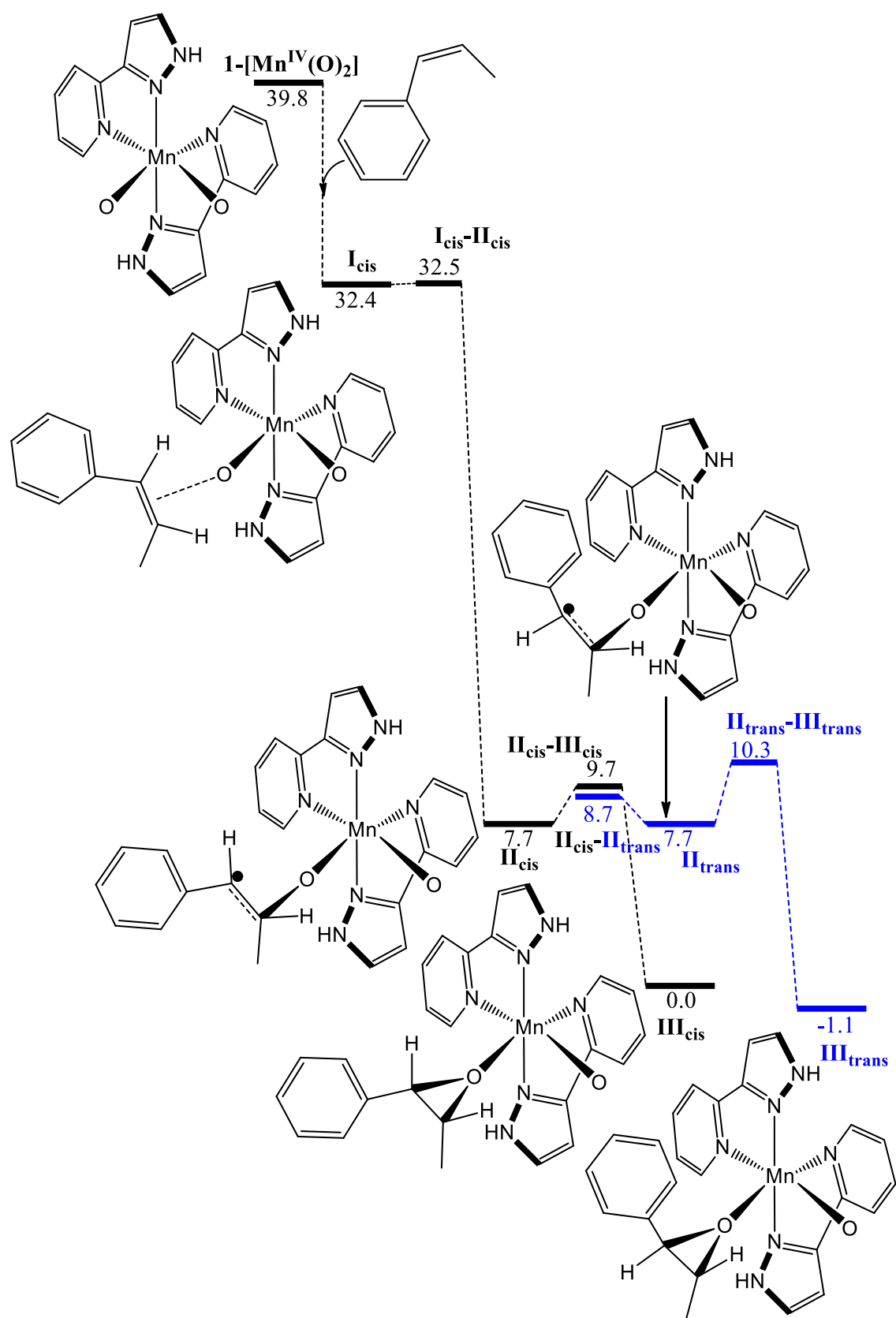
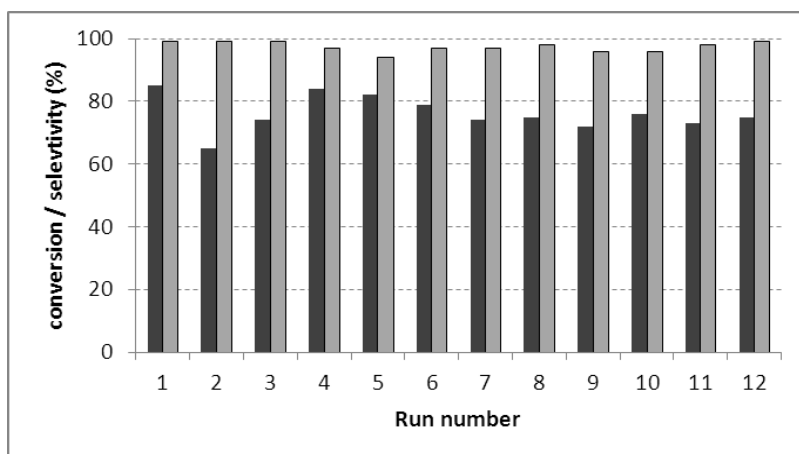
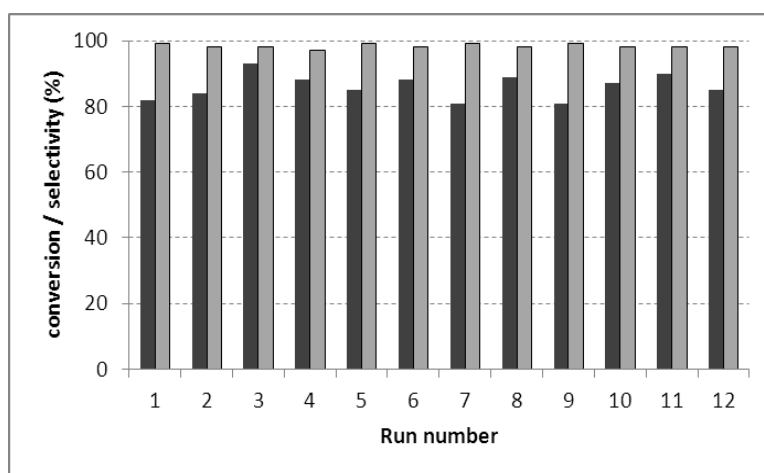


Figure 4.

a)



b)



References

- ¹ a) R. A. Sheldon and J. K. Kochi, in *Metal Catalyzed Oxidation of Organic Compounds*, Academic Press, New York, 1981; b) P. Gamez, P. G. Aubel, W. L. Driessen and J. Reedijk, *Chem. Soc. Rev.* 2001, **30**, 376-385; c) A. Robert and B. Meunier, in *Biomimetic Oxidations Catalyzed by Transition Metal Complexes*, ed. B. Meunier, Imperial College Press, 2000, Ch. 12; d) P. C. A. Bruijninx, G. van Koten and R. J. M. K. Gebbink, *Chem. Soc. Rev.* 2009, **37**, 2716-2744.
- ² a) S. Y. Ko, A. W. M. Lee, S. Masamune, L. A. Reed, K. B. Sharpless and F. J. Walker, *Science* 1983, **220**, 949-951; b) K. C. Nicolaou, N. Winssinger, J. Pastor, S. Ninkovic, F. Sarabia, Y. He, D. Vourloumis, Z. Yang, T. Li, P. Giannakakou and E. Hamel, *Nature* 1997, **387**, 268-272; c) S. D. Gagnon in *Encyclopedia of Polymer Science and Engineering*, 2nd ed. (Eds: H. F. Mark, N. M. Bikales, C. G. Overberger, G. Menges, J. I. Kroschwitz), John Wiley & Sons: New York, 1985, vol. 6, p. 273; d) D. J. Darensbourg, R. M. Mackiewicz, A. L. Phelps and D. R. Billodeaux, *Acc. Chem. Res.* 2004, **37**, 836-844; e) E. N. Jacobsen, *Catalytic Asymmetric Synthesis* (Ed: I. Ojima), VCH: New York, 1993, p. 229; f) G. De Faveri, G. Ilyashenko and M. Watkinson, *Chem. Soc. Rev.* 2011, **40**, 1722-1760.
- ³ a) K.-P. Ho, W.-L. Wong, K.-M. Lam, C.-P. Lai, T. H. Chan and K.-Y. Wong, *Chem. Eur. J.* 2008, **14**, 7988-7996; b) S. Groni, P. Dorlet, G. Blain, S. Bourcier, R. Guillot and E. Anxolabéhère-Mallart, *Inorg. Chem.* 2008, **47**, 3166-3172; c) G. Yin, A. M. Danby, D. Kitko, J. D. Carter, W. M. Scheper and D. H. Busch, *Inorg. Chem.* 2007, **46**, 2173-2180.
- ⁴ a) M. Gómez, G. Muller and M. Rocamora, *Coord. Chem. Rev.* 1999, **193**, 769-835; b) G. C. Hargaden and P. J. Guiry, *Chem. Rev.* 2009, **109**, 2505-2550.
- ⁵ a) A. von Zelewsky and O. Mamula, *J. Chem. Soc., Dalton Trans.* 2000, 219-231; b) G. Chelucci and R. P. Thummel, *Chem. Rev.* 2002, **102**, 3129-3170; c) J. Rich, M. Rodríguez, I. Romero, L. Vaquer, X. Sala, A. Llobet, M. Corbella, M.-N. Collomb and X. Fontrodona, *Dalton Trans.* 2009, 8117-8126; d) J. Rich, M. Rodríguez, I. Romero, X. Fontrodona, P. W. N. M van Leeuwen, Z. Freixa, X. Sala, A. Poater and M. Solà, *Eur. J. Inorg. Chem.* 2013, 1213-1224.
- ⁶ B. Meunier, *Chem. Rev.* 1992, **92**, 1411-1456.
- ⁷ a) M. Palucki, M. S. Finney, P. J. Pospisil, M. L. Güler, T. Ishida and E. N. Jacobsen, *J. Am. Chem. Soc.* 1998, **120**, 948-954; b) T. Katsuky, *Adv. Synth. Catal.* 2002, **344**, 131-147; c) P. G. Cozzi, *Chem. Soc. Rev.* 2004, **33**, 410-421.
- ⁸ J. Rich, E. Manrique, F. Molton, C. Duboc, M.-N. Collomb, M. Rodríguez and I. Romero, *Eur. J. Inorg. Chem.* 2014, 2663-2670; b) A. Murphy, A. Pace and T. D. P. Stack, *Org. Lett.*, 2004, 3119-3122; c) A. Murphy, G. Dubois, and T. D. P. Stack, *J. Molec. Catal.*, 2006, **251**, 78-88; d) J.T. Tracy and T. Daniel P. Stack *J. Am. Chem. Soc.*, 2008, **130** (14), 4945-4953.
- ⁹ a) M. Viciano-Chumillas, M. Giménez-Marqués, S. Tanase, M. Evangelisti, I. Mutikainen, U. Turpeinen, J. M. M. Smits, R. de Gelder, L. J. de Jongh and J. Reedijk, *J. Phys. Chem. C* 2008, **112**, 20525-20534; b) M. Viciano-Chumillas, S. Tanase, I. Mutikainen, U. Turpeinen, L. J. de Jongh and J. Reedijk, *Dalton Trans.* 2009, 7445-7453.
- ¹⁰ a) P. T. Anastas, J. C. Warner, *Green Chemistry: Theory and Practice*; Oxford University Press: Oxford, U.K., 1998; b) M. Lancaster, in *Handbook of Green Chemistry and Technology*; Clark, J. H.,

- Macquarrie, D. J., Eds.; Blackwell Publishing: Abingdon, U.K., 2002; c) M. Lancaster, *Green Chemistry: An Introductory Text*; RSC: London, 2002; d) M. Poliakoff, J. M. Fitzpatrick, T. R. Farren and P. T. Anastas, *Science*, 2002, **297**, 807-810; e) P. T. Anastas and M. Kirchhoff, *Acc. Chem. Res.* 2002, **35**, 686-694; f) R. A. Sheldon, *Green Chem.* 2005, **7**, 267-278; g) R. A. Sheldon, I. Arends and U. Hanefeld, *Green Chemistry and Catalysis*; Wiley-VCH: Weinheim, Germany, 2007.
- ¹¹ a) C.Capello, U. Fischer and K. Hungerbühler, *Green Chem.* 2007, **9**, 927-934; b) H. García-Marín, J. C. Van der Toorn, J. A. Mayoral, J.I. García, I. W.C.E. Arends, . C.Capello, U. Fischer and K. Hungerbühler, *Green Chem.* 2009, **11**, 1605-1609.
- ¹² a) D. Tavor, O. Sheviev, C. Dlugy and A. Wolfson, *Can. J. Chem.* 2010, **88**, 305-308; b) J. Francos and V. Cadierno, *Green Chem.* 2010, **12**, 1552-1555; c) S. Balieu, A. El Zein, R. De Sousa, F. Jérôme, A. Tatibouët, S. Gatard, Y. Pouilloux, J. Barrault, P. Rollin and S. Bouquillon, *Adv. Synth. Catal.* 2010, **352**, 1826-1833; d) A. E. Díaz-Álvarez, J. Francos, B. Lastra-Barreira, P. Crochet and V. Cadierno, *Chem. Commun.* 2011, **47**, 6208-6227; e) Y. Gu and F. Jérôme, *Green Chem.* 2010, **12**, 1127-1138; f) J. I. García, H. García-Marín, J. A. Mayoral and P. Pérez, *Green Chem.* 2010, **12**, 426-434.
- ¹³ H. García-Marín, J. C. van der Toorn, J. A. Mayoral, J. I. García and I. W.C. E. Arends, *J. Mol. Catal. A* 2011, **334**, 83-88.
- ¹⁴ a) G. Centi and S. Perathoner, in *Methods and Tools of Sustainable Industrial Chemistry: Catalysis, in Sustainable Industrial Chemistry* (Eds F. Cavani, G. Centi, S. Perathoner, F. Trifiró), Wiley-VCH Verlag GmbH & Co. KGaA, Weinheim, Germany, 2009, ch2; b) N. V. Plechkova and K. R. Seddon, *Chem. Soc. Rev.* 2008, **37**, 123-150.
- ¹⁵ Y. Liu, H. -J. Zhang, Y. Lu, Y. -Q. Cai and X.-L. Liu, *Green Chem.* 2007, **9**, 1114-1119.
- ¹⁶ a) H. -J. Zhang, Y. Liu, Y. Lu, X. -S. He, X. Wang and X. Ding, *J. Mol. Catal. A: Chem.*, 2008, **287**, 80-86; b) R. Tan, D. Yin, N. Yu, H. Zhao and D. Yin, *J. Catal.*, 2009, **263**, 284-291; c) J. Teixeira, A. R. Silva, L. C. Branco, C. A. M. Afonso and C. Freire, *Inorg. Chim. Acta*, 2010, **363**, 3321-3329; d) J. Muzart, *Adv. Synth. Catal.* 2006, **348**, 275-295.
- ¹⁷ K-P. Ho, W-L. Wong, L. Y. S. Lee, K.-M. Lam, T. H. Chan and K-Y Wong, *Chem. Asian J.* 2010, **5**, 1970-1973.
- ¹⁸ a) S. McCann, M. McCann, R. M. T. Casey, M. Jackman, M. Devereux and V. McKee, *Inorg. Chim. Acta* 1998, **279**, 24-29; b) C. Chen, H. Zhu, D. Huang, T. Wen, Q. Liu, D. Liao and J. Cui, *Inorg. Chim. Acta* 2001, **320**, 159-166; c) J. A. Smith, J. R. Galán-Masacrós, R. Clérac, J.-S. Sun, X. Ouyang and K. R. Dunbar, *Polyhedron* 2001, **20**, 1727-1734; d) C. Baffert, I. Romero, J. Pécaut, A. Llobet, A. Deronzier and M.-N. Collomb, *Inorg. Chim. Acta* 2004, **357**, 3430-3436; e) R.-Q. Zou, C.-S. Liu, X.-S. Shi, X.-H. Bu and J. Ribas, *Cryst. Eng. Comm.* 2005, **7**, 722-727; f) R. van Gorkum, F. Buda, H. Kooijman, A. L. Spek, E. Bouwman and J. Reedijk, *Eur. J. Inorg. Chem.* 2005, 2255-2261.
- ¹⁹ a) M. Karthikeyan, S. Karthikeyan and B. Manimaran, *Acta. Cryst. Sect. E* 2011, **67**, m1367; b) B. Hachula, M. Pedras, D. Petak, M. Nowak, J. Kusz and J. Borek, *Acta. Cryst. Sect. C* 2009, m215-m218; c) R. Kruszynski, T. J. Bartczak, A. Adamczyk, D. Czakis-Sulikowska and J. Kaluzna, *Acta. Cryst. Sect. E* 2001, **57**, m183-m185
- ²⁰ J. M. Lehn, *Supramolecular Chemistry*, VCH, Weinheim, 1995.

- ²¹ X. H. Bu, M. L. Tong, H. C. Chang, S. Kitagawa and S. R. Batten, *Angew. Chem., Int. Ed.* 2004, **43**, 192-195.
- ²² A.W. Addison, T. N. Rao, J. Reedijk, J. V. Rijn and G. C. Verschoor, *J. Chem. Soc., Dalton Trans.*, 1984, 1349-1356.
- ²³ C. Hureau, G. Blondin, M.-F. Charlot, C. Philouze, M. Nierlich, M. Césario and E. Anxolabéhère-Mallart, *Inorg. Chem.* 2005, **44**, 3669–3683.
- ²⁴ I. Romero, M.-N. Collomb, A. Deronzier, A. Llobet, E. Perret, J. Pecaut, L. Le Pape and J. M. Latour, *Eur. J. Inorg. Chem.* 2001, 69-72.
- ²⁵ a) M. U. Triller, D. Pursche, W.-Y. Hsieh, V. L. Pecoraro, A. Rompel and B. Krebs, *Inorg. Chem.* 2003, **42**, 6274–6283; b) M. Pascaly, M. Duda, A. Rompel, B. H. Sift, W. Meyer-Klaucke and B. Krebs, *Inorg. Chim. Acta* 1999, **291**, 289–299; c) C. Mantell, H. Y. Chen, R. H. Crabtree, G. V. Brudvig, J. Pecaut, M.-N. Collomb and C. Duboc, *Chem. Phys. Chem.* 2005, **6**, 541–546; d) R. Dingle, *Acta Chem. Scand.* 1966, **20**, 33–44; e) T. S. Davis, J. P. Fackler and M. J. Weeks, *Inorg. Chem.* **1968**, *7*, 1994–2002.
- ²⁶ M. Sankaralingam and M. Palaniandavar, *Dalton Trans.* 2014, **43**, 538-550.
- ²⁷ a) B. Kan, M. Kim, J. Lee, Y. Do and S. Chang, *J. Org. Chem.* 2006, **71**, 6721-6727. b) I. García-Bosch, A. Company, X. Fontrodona, X. Ribas, and M. Costas. *Org. Lett.* 2008, **10**, 2095-2098.
- ²⁸ a) W. Adam, K. J. Roschmann, C. R. Saha-Möller and D. J. Seebach, *J. Am. Chem. Soc.* 2002, **124**, 5068-5073; b) S.-E. Park, W. J. Song, Y. O. Ryu, M. H. Lim, R. Song, K. M. Kim and W. J. Nam, *J. Inorg. Biochem.* 2005, **99**, 424-431.
- ²⁹ a) S. H. Lee, L. Xu, B. K. Park, Y. V. Mironov, S. H. Kim, Y. J. Song, C. Kim, Y. Kim and S.-J. Kim, *Chem. Eur. J.* 2010, **16**, 4678–4685; b) R. V. Ottenbacher, K. P. Bryliakov and E. P. Talsi, *Inorg. Chem.* 2010, **49**, 8620–8628.
- ³⁰ a) G. Yin, M. Buchalova, A. M. Danby, C.M. Perkins, D. Kitko, J. D. Carter, W. M. Scheper and D. H. Busch, *J. Am. Chem. Soc.*, 2005, **127**, 17170-17171; b) G. Yin, A. M. Danby, D. Kitko, J. D. Carter, W. M. Scheper and D. H. Busch, *J. Am. Chem. Soc.*, 2008, **130**, 16245-16253.
- ³¹ a) N. Jin, M. Ibrahim, T. G. Spiro and J. T. Groves, *J. Am. Chem. Soc.*, 2007, **129**, 12416-12417; b) W. Liu and J. T. Groves, *J. Am. Chem. Soc.*, 2010, **132**, 12847-12849.
- ³² M. Ferbert, F. Montilla, A. Galindo, R. Moyano, A. Pastor and E. Alvarez, *Dalton Trans.* 2011, **40**, 5210-5219.
- ³³ a) J. C. Ma and D. A. Dougherty, *Chem. Rev.* 1997, **97**, 1303-1324; b) C. G. Hanke, A. Johansson, J. B. Harper and R. M. Lynden-Bell, *Chem. Phys. Lett.* 2003, **374**, 85-90; c) H. Olivier-Bourbigou, L. Magna and D. Morvan, *Appl. Catal. A* 2010, **373**, 1-56; d) V. I. Pârvulescu and C. Hardadre, *Chem. Rev.* 2007, **107**, 2615-2665.
- ³⁴ a) J. Rudolph, K. L. Reddy, J. P. Chiang and K. B. Sharpless, *J. Am. Chem. Soc.* 1997, **119**, 6189-6190; b) H. Adolfsson, A. Converso and K. B. Sharpless, *Tetrahedron Lett.* 1999, **40**, 3991-3994.
- ³⁵ H. Brunner and T. Scheck, *Chem. Ber.* 1992, **125**, 701-709.
- ³⁶ Y. Inada, Y. Nakano, M. Inamo and S. Funashashi, *Inorg. Chem.* 2000, **39**, 4793-4801.
- ³⁷ J. Catalán, F. Fabero, R. M. Claramunt, M. D. Santa María, M. C. Foces-Foces, F. Hernández, M. Martínez-Ripoll, J. Elguero and R. Sastre, *J. Am. Chem. Soc.* 1992, **114**, 5039-5048.

³⁸ Gaussian 09, Revision A.1, M. J. Frisch, G. W. Trucks, H. B. Schlegel, G. E. Scuseria, M. A. Robb, J. R. Cheeseman, G. Scalmani, V. Barone, B. Mennucci, G. A. Petersson, H. Nakatsuji, M. Caricato, X. Li, H. P. Hratchian, A. F. Izmaylov, J. Bloino, G. Zheng, J. L. Sonnenberg, M. Hada, M. Ehara, K. Toyota, R. Fukuda, J. Hasegawa, M. Ishida, T. Nakajima, Y. Honda, O. Kitao, H. Nakai, T. Vreven, J. A. Montgomery, Jr., J. E. Peralta, F. Ogliaro, M. Bearpark, J. J. Heyd, E. Brothers, K. N. Kudin, V. N. Staroverov, R. Kobayashi, J. Normand, K. Raghavachari, A. Rendell, J. C. Burant, S. S. Iyengar, J. Tomasi, M. Cossi, N. Rega, N. J. Millam, M. Klene, J. E. Knox, J. B. Cross, V. Bakken, C. Adamo, J. Jaramillo, R. Gomperts, R. E. Stratmann, O. Yazyev, A. J. Austin, R. Cammi, C. Pomelli, J. W. Ochterski, R. L. Martin, K. Morokuma, V. G. Zakrzewski, G. A. Voth, P. Salvador, J. J. Dannenberg, S. Dapprich, A. D. Daniels, Ö. Farkas, J. B. Foresman, J. V. Ortiz, J. Cioslowski, D. J. Fox, Gaussian, Inc., Wallingford CT, 2009.

³⁹a) Y. Zhao and D. G. Truhlar, *J. Chem. Phys.* 2006, **125**, 194101-194118; b) Y. Zhao and D. G. Truhlar, *Theor. Chem. Acc.* 2008, **120**, 215-241.

⁴⁰A. Schaefer, H. Horn and R. Ahlrichs, *J. Chem. Phys.* 1992, **97**, 2571-2577.

⁴¹a) U. Haeusermann, M. Dolg, H. Stoll and H. Preuss, *Mol. Phys.* 1993, **78**, 1211-1224; b) W. Kuechle, M. Dolg, H. Stoll and H. Preuss, *J. Chem. Phys.* 1994, **100**, 7535-7542; c) T. Leininger, A. Nicklass, H. Stoll, M. Dolg and P. Schwerdtfeger, *J. Chem. Phys.* 1996, **105**, 1052-1059.

⁴²a) V. Barone and M. Cossi, *J. Phys. Chem. A* 1998, **102**, 1995-2001; b) J. Tomasi and M. Persico, *Chem. Rev.* 1994, **94**, 2027-2094.

